Sensor Array Optimization for Seismic Estimation via Structured Sparse Inversion

Sérgio M. Jesus

LARSyS, University of Algarve, Campus de Gambelas
8005-139 Faro, Portugal
Email: sjesus@ualg.pt

Abstract—This paper presents a distributed sensor array optimization algorithm for Autonomous Underwater Vehicles (AUV)-based seismic surveying. The algorithm is based on a sparse formulation of bottom layer reflection resulting on a structured design matrix with the bottom return field. Since the design matrix structure depends also on the receiving system characteristics, field coherence is used as optimization criteria for determining sensor array position. The receiver positions are constrained by actual array characteristics and AUV relative position physical constraints. Simulated results based on actual physical propagation model data are provided for a three AUV 1D geometry case. These results show that a clear improvement can be reached regarding bottom layer resolution in depth and range. The developed methodology may be useful for the resource planning and setup of seismic surveying experiments involving moving sensing arrays such as those under test in the EU WiMUST project[1].

I. INTRODUCTION

Estimating ocean bottom properties poses a number of scientific and technological challenges because the media is largely anisotropic and of difficult or impossible direct access. The fulfillment of generic requirements of bottom resolution has led to the development of large survey systems and associated seismic profiling techniques routinely used in the oil & gas industry since the 70's [1], [2]. These systems, composed of a bank of powerful sound sources and several km long streamers are costly, to develop, maintain and operate at sea.

The ongoing European project Widely Scalable Mobile Underwater Sonar Technology (WiMUST) proposes to replace the traditional ship towed survey system by a fleet of Autonomous Underwater Vehicles (AUV) towing short arrays of sensors [3]. This particular hardware setup brings a new dimension to the problem by physically decoupling the acoustic source and the receiver system and by allowing the receivers to move (almost) freely relative to each other and to the source, creating an effective Distributed Sensor Array (DSA). Whether this "freedom" allows to reach new gains in terms of performance and adaptivity for determining the sub-bottom structure is a challenging question. More specifically, this paper focuses on determining and testing a suitable criteria for DSA geometry optimization in realistic ocean bottom survey scenarios.

One of the most popular approach is the Full Waveform Inversion (FWI) technique, proposed more than 30 years ago (a

recent state of the art account of FWI can be found in [4] and a detailed overview in [5]). FWI is a full-field approach that incorporates many of the details and estimation capabilities of the method described herein. FWI represents a challenge for seismic inversion in terms of both the large amount of data to handle and the complex numerical solving techniques it involves. Several approaches have been proposed to mitigate these difficulties among which one that realizes that seismic data in general allows to integrate sparsity constraints without a loss on parameter estimation accuracy [6]–[8]. Understanding sparsity allows to decrease data flow in terms of shot data and frequency bins according to estimation needs [9], [10] while keeping a faster convergence to the same or better solution. Compressive sensing (CS), or the ability to retrieve sparse information from large data sets, has been handled by randomizing source firing both in time and in frequency [11]–[13] with real data examples shown in [14]. To our knowledge CS has not been applied to the sensor space domain for sub-bottom inversion purposes.

The approach taken here is based on the minimization of the acoustic field coherence as calculated through a numerical model conditioned on *a priori* environmental information and system characteristics for any actual experiment and area at hand. Field coherence is then explored through CS of structured observation matrices for obtaining a sparse estimate of bottom layering. The setup is first characterized by a few performance tests and then results are obtained for the optimization of a three AUV 8 m towed array system in a shallow water simulated scenario showing a clear enhancement relative to the non-optimized array geometry.

This paper is organized as follows: the seismo-acoustic data model is described in section II; section III introduces compressive sensing in the sensor space and field coherence applied to the seismo-acoustic data model for DSA geometry optimization. Results obtained on synthetic data and conclusions are given in sections IV and V, respectively.

II. SEISMO-ACOUSTIC DATA MODEL

A seismo-acoustic propagation data model allows, in principle, to appropriately treat the interaction between bottom and sub-bottom layers, according to its specific physical properties (if they are known or assumed). The reflected acoustic field, observed at location $\mathbf{r}_k$ due to a unit amplitude monochromatic point source located at $\mathbf{r}_s$ may be written using the Green function $G(\cdot)$, harmonic solution at frequency ω of the Helmholtz

equation between two points in space, as

$$G^R(\mathbf{r}_k, \mathbf{r}_s) = \sum_{i=1}^{I} a_i G(\mathbf{r}_k, \mathbf{r}_i) G^I(\mathbf{r}_i, \mathbf{r}_s), \qquad k = 1, \ldots, K. \tag{1}$$

where $G(\mathbf{r}_k, \mathbf{r}_i)$ is the Green function between reflector located at bottom position $\mathbf{r}_i$ and sensor at $\mathbf{r}_k$, $G^I(\mathbf{r}_i, \mathbf{r}_s)$ is the bottom incident field at $\mathbf{r}_i$ from the sound source at location $\mathbf{r}_s$, a_i is the complex amplitude coefficient of the i-th reflector assumed random distributed and finally I is the number of effective reflectors. Using scattering is unnecessary in our application and, in any case the Born approximation would allow for the linearization of the interscatterer excitation field (the so-called Foldy-Lax system, see details in [15]) so the end result would be equivalent to (1). At this point our bottom reflected observation at receiver k, due to source shot $\mathbf{s}_l$ in noise $\mathbf{u}$ is

$$\hat{\mathbf{y}}_k(\boldsymbol{\theta}; l) = \mathbf{H}_{kl}(\boldsymbol{\theta})\mathbf{s}_l + \mathbf{u}_k(l), \tag{2}$$

where $\boldsymbol{\theta}$ is the bottom parameter vector to be determined and the impulse response in matrix $\mathbf{H}_{kl}(\boldsymbol{\theta})$ is given by the discrete inverse Fourier transform of the right hand side of (1) with the appropriate location vectors $\mathbf{r}_k$ and $\mathbf{r}_l$ defined for the k-th sensor and l-th source shot positions

$$h_{kl}(n) = \frac{1}{2\pi} \int_{\omega} \sum_{i=1}^{I} a_i G(\omega; \mathbf{r}_k, \mathbf{r}_i) G^I(\omega; \mathbf{r}_i, \mathbf{r}_l) e^{j\omega n T_s} d\omega, \tag{3}$$

where T_s is the sampling interval and the a_i are assumed frequency independent.

III. DSA GEOMETRY OPTIMIZATION

A. Compressed sensing in the sensor space

The importance of (1) is that it establishes a link between the target and the receiver domain by means of the appropriate Green functions. A full discretization of the sub-bottom into $M = M_1 \times M_2$ samples along a depth-range grid, where only a reduced number of grid points have effective reflectors, allows to cast the inverse problem into a sparse system of equations under the form

$$\mathbf{g} = \mathcal{G}\mathbf{x}, \tag{4}$$

where

- $\mathbf{g} = G^R(\mathbf{r}_k, \mathbf{r}_s)$ is a vector $J \times 1$
- matrix $\mathcal{G} = G(\mathbf{r}_j, \mathbf{r}_m) G^I(\mathbf{r}_m, \mathbf{r}_s)$ is $J \times M$, where the vectors $\mathbf{r}_m; i = 1, \ldots, M$ span the sub-bottom target domain, $\mathbf{r}_j; j = 1, \ldots, J$ span the sensor space domain, $\mathbf{r}_s$ is the source vector and
- $\mathbf{x}$ is a $M \times 1$ vector that is all zeros but for values $a_i, i = 1, \ldots, I$ of effective reflectors, so it is I-sparse.

So, for $I \ll M$, (4) represents a sparse system. Determining an accurate estimate $\hat{\mathbf{x}}$ of $\mathbf{x}$ would allow to obtain an estimate $\hat{I}$ of the number of effective reflectors I as the non zero values of $\hat{\mathbf{x}}$ and an estimate $\hat{a}_i$ of its relative reflection.

A tractable solution of (4) using a l_1-norm minimization algorithm will mainly depend on the mutual coherence and/or on the Restricted Isometry Property (RIP) of matrix $\mathcal{G}$. Since $\mathcal{G}$ is a matrix that depends on the Green functions of the media

between source - bottom - receiver and its physics related, the achievement of the RIP can not be guaranteed. The proposed solution allowing to decrease the mutual coherence without changing the observation matrix is based on the randomization of the rows of matrix $\mathcal{G}$ [16]. This is done by observing vector $\mathbf{g}$ by a channel sampling matrix $\tilde{\mathbf{\Phi}}$ of dimension $K \times J$, for $K \ll J$, and where each row of $\tilde{\mathbf{\Phi}}$ will have a single 1 at a random position among the J columns. Thus we can form the observation $\mathbf{y}$,

$$\begin{aligned} \mathbf{y} &= \tilde{\mathbf{\Phi}}\mathbf{g}, \\ &= \tilde{\mathbf{\Phi}}\mathcal{G}\mathbf{x}, \\ &= \mathbf{A}\mathbf{x} \end{aligned} \tag{5}$$

where now $\mathbf{A} = \tilde{\mathbf{\Phi}}\mathcal{G}$, of dimensions $K \times M$ with $K \ll M$ and with $\|x\|_0 = I^2$, and $I \ll K$, forming a sparse system of equations. The mutual coherence $\mu(\mathbf{A})$ defined as

$$\mu(\mathbf{A}) = \max_{j,k=1,M} \frac{| < \mathbf{a}_j, \mathbf{a}_k > |}{\|\mathbf{a}_j\| \|\mathbf{a}_k\|}, \tag{6}$$

should verify the *Welch bound* [17] given by

$$\sqrt{\frac{M-K}{K(M-1)}} \leq \mu(\mathbf{A}) \leq 1. \tag{7}$$

There is, however, no guarantee that a solution can be reached through

$$\min_{\mathbf{x} \in \mathbb{R}^M} \|\mathbf{x}\|_1 \qquad s.t. \qquad \mathbf{A}\mathbf{x} = \mathbf{y} \tag{8}$$

although a solution is attainable with high probability when $\mu(\mathbf{A})$ is low. So, coherence plays an important role in CS. An interesting result mentioned in [18], [19] gives the required number of measurements K for a given sparsity level I, bounded by the coherence $\mu(\mathbf{A})$, as

$$K \geq c\mu^2(\mathbf{A}) I \log M. \tag{9}$$

where c is some positive constant. It can be easily seen that for moderate coherence, a low number of K measurements 20 to 40, per resolvable layer I may be used, almost independently from the required number of discretization samples. This is the reason why CS is essentially devoted to low coherence measurements, where the "compression gain" is most prominent. Relation (9) gives a figure and a more exact meaning to the statement "small coherence" and therefore to the degree of "flatness" required for matrix $\mathbf{A}$. A matrix with high coherence will have high "peaks" and deep "valleys" and a low probability to succeed in the inversion of a low I-sparse signal. Conversely, a well distributed matrix with dispersed small values all over its rows and columns, will show a low coherence and therefore a high probability for observing (and then inverting) for a low I-sparse signal. A high coherence observation would require that the information is concentrated on a few points, one would say that the **diversity is low**, instead, in a low coherence observation the information is spread out and the **diversity is said to be high**. The idea behind DSA geometry optimization is to determine the sensor placement that minimizes the mutual coherence $\mu(\mathbf{A})$, of course, conditioned on the operational restrictions imposed by the system constraints and on the a priori knowledge of the environmental conditions of the test site.

---

[2] the l_0-norm is used as the number of non-zero values of vector $\mathbf{x}$.

IV. RESULTS ON SIMULATED DATA

A. Simulation scenario

The simulation scenario is intended to mimic the environment of the geophysical survey carried out in June 2015 in the area of Peljesac (Croatia). The environmental parameters are shown in table **??**. In this canonical scenario the source is considered to be explosive, located at 0.3m depth and emitting in the band 700 - 2000 Hz. Figure 1 shows a OASES

TABLE I: Peljesac canonical scenario OASES model parameters: C_p-compressional velocity, C_s shear velocity, α_p compressional attenuation, α_s shear attenuation and ρ density.

Layer	Depth (m)	C_p (m/s)	C_s (m/s)	α_p (dB/λ)	α_s (dB/λ)	ρ (g/cm^3)
water		1500	0	0	0	1
sed 1	30	1550	130	0.1	1.7	1.49
sed 2	38	1700	350	0.8	2.0	1.88
bottom	48	2500	900	0.01	0.01	2.4

model generated transmission loss (TL) at 1350 Hz (a) and the channel impulse response (CIR) in the band 700-2000 Hz for the full array aperture (b), in the canonical conditions of table **??**. Several remarks can be made for plot (a): i)
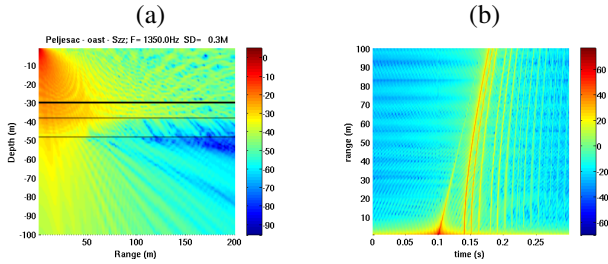

Fig. 1: Peljesac canonical scenario: OASES transmission loss at 1350 Hz (a) and CIR for the full array aperture in the band 700-2000 Hz (b).

at high grazing angles (near vertical) bottom penetration is high and sound covers all the layers down to the sub-bottom half space; ii) at approximately 50 m range the half space cut-off angle is attained and the penetration reaches only the second bottom layer, this happens until approximately 80 m horizontal range; iii) beyond that range, most of the energy reaches only the first sediment layer that has approximately the same compressional sound speed than the water column, and then propagates through it, eventually bouncing back to the water column at longer range. In the time-range plot of Figure 1(b), the curvature of the bottom arrival structure can clearly be seen for variable offset. At close range the field is dominated by the direct-surface reflect paths. Due to the close distance to the surface, a dipole behavior is observed canceling out with time/range. The packs of bottom returns can be clearly seen fading out as the number of bounces increases.

B. DSA geometry optimization

The solution of model (5) for obtaining an estimate $\hat{\mathbf{x}}$ of layer reflectance $\mathbf{x}$ requires

$$\hat{\mathbf{x}} = \arg\min_{\mathbf{x} \in \mathbb{R}^M} \|\mathbf{x}\|_1 \quad \text{s.t.} \quad \|\mathbf{A}\mathbf{x} - \mathbf{y}\|_2 \leq \delta \qquad (10)$$

with $\delta = 0.1$ for the l_2 constrained part, which was shown to provide a good compromise between speed and stability[3]. Other minimization alternatives could be possible, including those with regularizers such as OSCAR [20] or OWL [21], known to better handle correlated design matrices. The coherence $\mu(\mathbf{A})$ of matrix $\mathbf{A}$ will be watched closely since it will be determinant for the solver to provide a stable solution.

Based on the stylized Peljesac environment, a 2D range-depth-dependent sub-bottom scenario was generated by setting the values of coefficients a_i along a stretch of 80×60 m with a sub-bottom discretization of 1m. The number of effective sensors used for the inversion was 40. This number was chosen to represent a deployment of 5 AUVs with a 8 sensors streamer at 1m spacing each. The 40 sensors were randomly chosen among the 100 positions initially calculated. The result for this canonical environment for a monochromatic wave at 1350 Hz, is shown in Figure 2(a) and for a signal-to-noise ratio (SNR) of 0 dB (b). The estimated coherence of the 40×80 matrix is in the range [0.90,0.95] and, of course, varies with each realization. The clutter seen in the sparse vector estimate for 0
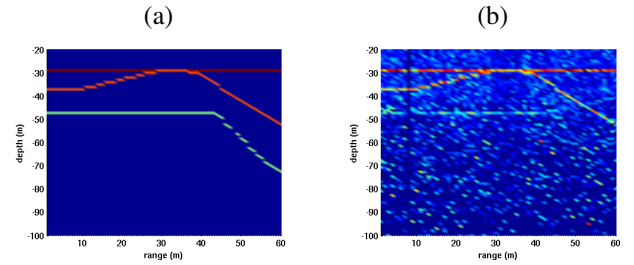

Fig. 2: sub-bottom l_1-norm estimate with BP algorithm in the Peljesac environment for the range dependent canonical scenario (a) and with a SNR of 0 dB (b).

dB SNR is sufficient to shadow some of the deeper reflectors and/or significantly change its contrast.

1) The effect of the number of sensors and array aperture: Varying the number of sensors and the array aperture are related but not equivalent. In linear array processing the spatial sampling rate relates to the maximum reachable frequency before aliasing, while array aperture, or the physical array length, defines the maximum attainable resolution, or the ability to discriminate closely spaced targets. In our case, array aperture relates more to diversity and observability of bottom features. In this test the number of sensors was kept constant at K=40, and the aperture was progressively increased in the following steps: 50, 100, 200, 400 and 500m. The coherence of the observation matrix decreases with increasing aperture as shown in Figure 3(a). This effect is equivalent to and agrees with that reported in [22]. Although in the 500m aperture the coherence is low, the bottom bearing information signal received in sensors placed 500m away from the estimation point have very low information of the deeper layers as seen in the transmission loss Figure 1(b). This justifies the poor identification of the deeper layer in Figure 3(b).

2) Geometry optimization: The objective of the DSA geometry optimization procedure is to maximize diversity by
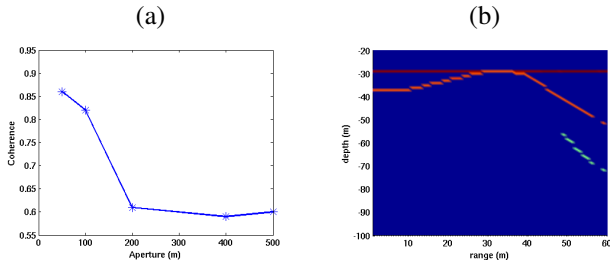

Fig. 3: observation matrix coherence for 40 sensors at 1350 Hz and variable array aperture (a) sub-bottom l_1-norm estimate for the range dependent Peljesac environment with 40 sensors in 500m aperture array (b).

changing sensor position and therefore attain a lower coherence within given constraints. This optimization was carried with Genetic Algorithm (GA) for minimizing the mutual coherence of a given design matrix according to (6). The various GA configuration parameters are given in the table of Figure 4(a). The GA convergence results for this case are shown in Figure 4(b) for the cost function evolution through iteration of the best individual and for the population mean (upper plot) and the final best individual (lower plot). **Distributed**
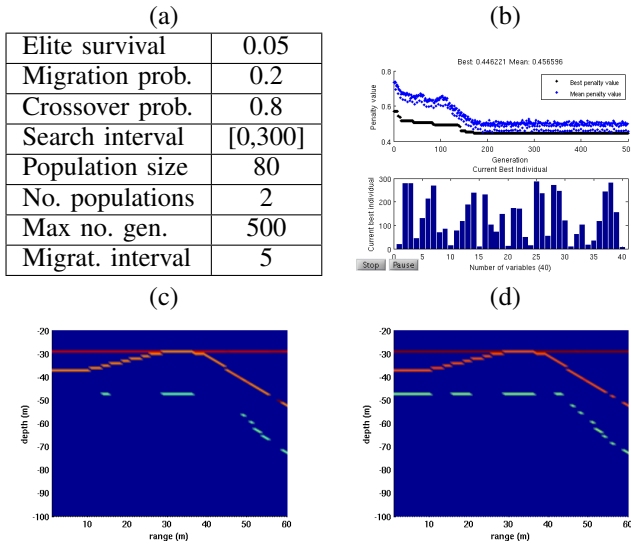

Fig. 4: DSA optimization for 1350 Hz, L=300 and K=40: with GA parameters given in (a), GA convergence shown in (b) and obtaining the sub-bottom l_1-norm estimate with constrained l_1 norm minimization in the Peljesac environment without optimization (c) and after optimization (d).

array case: we will assume that the linear array is formed by K=40 sensors distributed in a possible horizontal line of 300m at 1m spacing slots (L=300). A monochromatic frequency of 1350 Hz was used. The sub-bottom reflectors estimate obtained for the RD case is shown in Figure 4 for the case without optimization (c) and with GA optimization (d). The coherence was decreased from 0.78 to 0.43 which brought a better definition for the deeper reflectors.

AUV-based array case: let us now get a little bit closer to the problem at hand, that is to place a given number of AUVs in the terrain so as to optimize the sub-bottom inversion. Let us assume in this example that we have N_{auv}=3, each equipped with a streamer of 8 hydrophones at 1m spacing. For the time being the placement of the AUVs will be restricted to the 1D array case. The comparison of the reflector estimate results with a random placement of the AUVs and an optimized placement is shown in Figure 5. During the optimization the coherence was reduced from 0.88 to 0.73 and, as in the previous case, a better definition in the second and third line of reflectors at the deeper locations was obtained. After optimization the AUVs were located at 28, 73 and 185 m from the sound source.
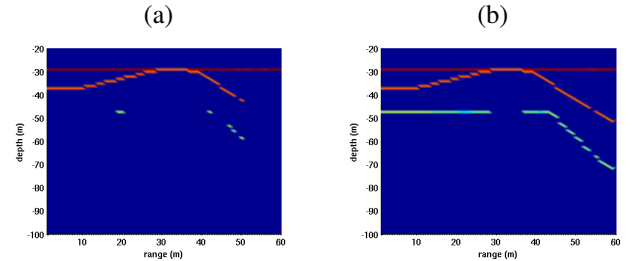

Fig. 5: DSA optimization for 1350 Hz, L=300 and Nauv=3 equipped with a 8 hydrophone streamer each (K=24): sub-bottom l_1-norm estimate in the Peljesac environment without optimization (a) and after GA optimization (b).

V. CONCLUSION AND NEXT DEVELOPMENTS

The problem of determining sensor position for observing a set of physical properties in a unknown scenario is, in general, ill-posed. Closed form solutions are possible only for very particular cases of analytically resolvable scenarios or for highly constrained geometries which, in most cases, are not interesting for practical applications. Optimal positioning of AUVs in the WiMUST scenario is a typical example of such an ill-posed problem.

The proposed cost function for geometry optimization is based on the acoustic field coherence to be minimized for the constrained array sensor geometry. In this setting the problem is viewed as determining an estimate of a sparse vector whose most significant entries are the location of the relevant bottom reflectors. This falls into the area of compressed sensing applied, in this case, in the sensor array space. Minimizing the coherence of the acoustic field for a simulated scenario based on *a priori* information is demonstrated for a linear (1D) array both for scattered sensors and for groups of small linear arrays, aiming to represent the streamers carried by the AUVs. In both cases the results show that sensor array optimization leads to a better detection of deeper reflectors.

REFERENCES

[1] O. Yilmaz, *Seismic data processing*. Tulsa: SEG, 1987.

[2] R. Sheriff and L. Geldart, *Exploration Seismology*. Cambridge, UK: Cambridge university Press, 1995.

[3] H. Al-Khatib, G. Antonelli, A. Caffaz, A. Caiti, I. B. d. J. G. Casalino, H. Duarte, G. Indiveri, S. Jesus, K. Kebkkal, A. Pascoal, and D. Polani, "The widely scalable mobile underwater sonar technology (wimust) project: an overview," in *MTS/IEEE Oceans'15*, Genova, Italy, 2015.

[4] J. Brittan, J. Bai, H. Delome, C. Wang, and D. Yingst, "full waveform inversion - the state of the art," *EAGE First Break*, vol. 31, pp. 75–81, October 2013.

[5] J. Virieux and S. Operto, "An overview of full-waveform inversion in exploration geophysics," *Geophysics*, vol. 74, no. 6, pp. WCC1–WCC26, November-December 2009. [Online]. Available: http://dx.doi.org/10.1190/1.3238367

[6] J. Charléty, S. Voronin, G. Nolet, I. Loris, F. Simons, K. Sigloch, and I. Daubechies, "Global seismic tomography with sparsity constraints: comparison with smoothing and damping regularization," *J. Geophys. Res. Solid Earth*, vol. 118, pp. 1–13, 2013. [Online]. Available: http://dx.doi.org/10.1002/jgrb.50326

[7] L. Zhu, E. Liu, and J. McClellan, "Fast online orthonormal dictionary learning for efficient full waveform inversion," in *IEEE ICASSP 2016*, Shangai, China, March 2016.

[8] F. Herrmann, "Sub-nyquist sampling and sparsity: how to get more information from fewer samples," in *Proc. Soc. Exploration Geophysicists Annual Meeting*, Houston, US, October 2009, pp. 3410–3415.

[9] P. Moghaddam and F. Herrmann, "Randomized full-waveform inversion: a dimensionality-reduction approach," in *SEG Technical Program Expanded Abstracts*, vol. 29, 2010, pp. 977–982.

[10] F. Herrmann, I. Hanlon, R. Kumar, T. van Leeuwen, X. Li, B. Smithyman, H. Watson, A. Calvert, M. Javanmehri, and E. Takougang, "Frugal full-waveform inversion: from theory to a practical algorithm," *SEG - The Leading Edge*, vol. 32, no. 9, pp. 1082–1092, September 2013.

[11] H. Mansour, H. Watson, T. Lin, and F. Herrmann, "A compressive sensing perspective on simultaneous marine acquisition," in *Proc. 20th Conf. of the Brazilian Geophysical Soc.*, Rio de Janeiro, Brasil, August 2011.

[12] ——, "Randomized marine aquisition without simultaneous sourcing," University of British Columbia, Technical Report TR-2011-04, January 2012.

[13] H. Mansour, F. Herrmann, and O. Yilmaz, "Improved wavefield reconstruction from randomized sampling via weighted one-norm minimization," *J. Int. Geophysics*, vol. 201, pp. 1182–1194, May 2015.

[14] C. Mosher, E. Keskula, S. Kaplan, R. Keys, C. Li, E. Ata, L. Morley, J. Brewer, F. Janiszewaki, P. Eick, R. Olson, and S. Sood, "Compressive seismic imaging," in *SEG Annual meeting*, Las Vegas, USA, 2012.

[15] K. Huang, K. Solna, and H. Zhao, "Generalized Foldy-Lax formulation," *J. Comput. Physics*, vol. 229, pp. 4544–4553, 2010.

[16] S. Jesus, "Distributed sensor array for bottom inversion," in *IEEE/OES China Ocean Acoustics COA'2016*, Harbin, China, January 2016.

[17] L. Welch, "Lower bounds on the maximum cross-correlation of signals," *IEEE Trans. on Information Theory*, vol. 20, no. 3, pp. 397–399, 1974.

[18] E. Candès and J. Romberg, "Sparsity and inchoerence in compressive sampling," *Inverse Problems*, vol. 23, pp. 969–985, 2007.

[19] E. Candès and M. Wakin, "An introduction to compressive sampling," *IEEE Signal Processing Magazine*, vol. 25, no. 3, pp. 21–30, March 2008.

[20] H. Bondell and B. Reich, "Simultaneous regression shrinkage, variable selection, and supervised clustering of predictors with oscar," *Biometrics*, vol. 64, pp. 115–123, 2007.

[21] M. Figueiredo and R. Novak, "Sparse estimation with strongly correlated variables using ordered weighted l1 regularization," *Eprint arXiv*, p. 1409.4005, 2014.

[22] A. Fannjiang, P. Yann, and T. Strohmer, "Compressed remote sensing of sparse objects," *arXiv:0904-3994*, 2009.